

# Practical strategies for the solution of large-scale electromagnetic inverse problems

Douglas W. Oldenburg

Geophysical Inversion Facility, Department of Geophysics and Astronomy  
University of British Columbia, Vancouver, Canada

**Abstract.** Nonlinear inverse problems in electromagnetics are typically solved by dividing the Earth into cells of constant conductivity, linearizing the equations about a current model, computing the sensitivities, and then solving an optimization problem to obtain an updated estimate of the conductivity. In principle, this procedure can be implemented for any size problem, but in practice the computations involved may be too large for the available computing hardware. In electromagnetics this is currently the situation irrespective of whether the interpreter has access to a workstation or a supercomputer. In addition to the demands imposed by the need to compute the predicted responses from a specified model (i.e., invoking a forward mapping) there are two computational roadblocks encountered when solving an inverse problem: (1) calculation of the sensitivity matrix and (2) solution of the resultant large system of equations. If either of these operations cannot be carried out in reasonable time then an alternate strategy is required. Such strategies include generalized subspace methods, conjugate gradient methods, or approximate inverse mapping (AIM) procedures. The theoretical foundations and computational details of these strategies are explored in this paper with the ultimate goal that the inversionist, after assessing his/her computing power and knowing the time required to perform forward modeling, can generate a methodology by which to solve the problem. The methodologies are compared quantitatively by considering an archetypal inversion problem in electromagnetics, the inversion of dc potential data to recover the electrical conductivity.

## 1. Introduction

In a typical inverse problem we are provided with  $N$  data  $d_j^{\text{obs}}$ , some estimate of their uncertainties  $\epsilon_j$ , and mappings of the form  $d_j = \mathcal{F}_j[m]$  which express the relationship between the  $j$ th datum  $d_j$  and a model  $m$ . With the usual constitutive relationships, and assuming a harmonic time dependence  $e^{i\omega t}$ , the operator  $\mathcal{F}$  for electromagnetic problems, defined on a finite or infinite domain  $D$ , is specified by the equations

$$\nabla \times \mathbf{E} = -i\omega\mu\mathbf{H} + \mathbf{M}_s \quad (1)$$

$$\nabla \times \mathbf{H} = (\sigma + i\omega\epsilon)\mathbf{E} + \mathbf{J}_s$$

where  $\mathbf{E}$  and  $\mathbf{H}$  are the electric and magnetic field strengths due to imposed electric and magnetic current densities  $\mathbf{J}_s$  and  $\mathbf{M}_s$ . The sources on the right-hand side may be natural or artificial, and the

electromagnetic problem is solved by satisfying (1) subject to boundary conditions applied on  $\partial D$  of the form

$$\alpha(\hat{\mathbf{n}} \times \mathbf{U}) + \beta(\hat{\mathbf{n}} \times \hat{\mathbf{n}} \times \nabla \times \mathbf{U}) = \mathbf{S} \quad (2)$$

where  $\alpha, \beta$  are constants,  $\mathbf{S}$  is a surface magnetic or electric current, and  $\mathbf{U}$  can be either  $\mathbf{E}$  or  $\mathbf{H}$ . The parameters of interest in the inversion can be any combination of  $\mu, \epsilon$ , and  $\sigma$ , but in this paper only  $\sigma$  is assumed to be variable. The data may be individual field values or ratios of fields, such as impedances or admittances. They constitute constraints upon the model, which we denote generically by the symbol  $m$ , and in the inverse problem we attempt to find an  $m$  which acceptably reproduces these data. The fundamental difficulty is that of nonuniqueness; there are generally infinitely many models which adequately reproduce the observations. Practical inverse problems are therefore formulated by first designing a specific objective functional of the model and then minimizing this functional subject to the data constraints.

Copyright 1994 by the American Geophysical Union.

Paper number 94RS00746.  
0048-6604/94/94RS-00746\$08.00

The reality of inversion is the following. Any inversion methodology involves a sequence of decisions by the inverter so that a single model can be constructed. The main decision points concern the data to be inverted and the model objective function to be minimized. Processing and acquisition difficulties make it difficult in general to specify data and their error statistics. Yet when an inversion is carried out, the data, estimated errors, and desired fit criterion are specified at the outset and assumed fixed. The next major hurdle faced by the inversionist is to specify the model objective function to be minimized. Is a "blocky" or "smooth" model desired? Is there a base model and if so, what is it? If a final model is to be close to a base model and yet smooth, what is the relative ratio for these quantities? What are the additional multiplicative functions in the norm components needed to get desired results (e.g., progressively more lateral smoothing with increased depth)? Alteration of any of the above factors dictates that the data must be re-inverted. Consequently, a particular data set must ultimately be inverted not once, but many times, and practicality demands that the inversion be efficient.

General Gauss-Newton linearized solutions can, in principle, be used to solve electromagnetic (EM) problems in two and three dimensions. An example of this is the inversion of magnetotelluric data in two dimensions by *deGroot-Hedlin and Constable* [1990]. The practical issue, however, is the amount of computation required as the number of cells and data increases. The roadblocks are (1) forward modeling; (2) calculation of sensitivities; and (3) solution of a large matrix. As the size of the problem increases, the computational burdens in these areas are exacerbated and eventually the inverter tires of waiting for the output, even when he/she has access to a large computer.

This paper presents alternate methodologies for solving inverse problems. It is not meant to be a review of existing techniques but is a merely a perspective which focuses upon methods that we have used and developed at the University of British Columbia Geophysical Inversion Facility over the last few years. The paper begins with a general background to our approach of the inverse problem and illustrates the nonuniqueness inherent in EM inverse problems by introducing the dc resistivity problem which is a thematic example for this paper. Three inverse methods are then presented in order

of decreasing computational burden. They are a subspace approach which reduces the size of the matrix system to be inverted, a conjugate gradient method which obviates the need to compute and subsequently invert the full sensitivity matrix, and approximate inverse mapping methods which require only one forward modeling per iteration. The paper concludes with summary comments.

## 2. Basic Equations and Nonuniqueness in Inversion Results

The fundamental difficulty in solving the inverse problem is the nonuniqueness of the solution. Practical inverse problems are therefore formulated by first designing a specific objective functional of the model and then minimizing this functional subject to the data constraints. Generally, the objective function is tailored so that the solution from the inverse algorithm is "close" to a prespecified base model or reference model and also that the constructed model has "minimum structure" in some sense. A particularly useful objective function for a three-dimensional model in a Cartesian coordinate frame is

$$\begin{aligned} \phi_m(m) = & \alpha_s \int_{\text{vol}} w_s (m - m_0)^2 dv \\ & + \alpha_x \int_{\text{vol}} w_x \left( \frac{\partial(m - m_0)}{\partial x} \right)^2 dv \\ & + \alpha_y \int_{\text{vol}} w_y \left( \frac{\partial(m - m_0)}{\partial y} \right)^2 dv \\ & + \alpha_z \int_{\text{vol}} w_z \left( \frac{\partial(m - m_0)}{\partial z} \right)^2 dv \end{aligned} \quad (3)$$

In (3) the functions  $w_s$ ,  $w_x$ ,  $w_y$ , and  $w_z$  are specified by the user and the constants  $\alpha_s$ ,  $\alpha_x$ ,  $\alpha_y$ , and  $\alpha_z$  control the importance of closeness of the constructed model to the base model  $m_0$  and control the roughness of the model in the three directions. The reference model can be omitted from the derivatives terms in (3) if desired. Pragmatic issues generally force us to parameterize the model as

$$m = \sum_{i=1}^M m_i \psi_i \quad (4)$$

where  $\psi_i$  are basis functions defined on  $D$  and  $m_i$  are constants. In this paper the basis functions are chosen to be rectangular prisms of unit amplitude, and hence  $m_i$  is the value of the model in the  $i$ th cell. Because our intent is to find a model which minimizes a specific objective function, the inversion results should not depend upon the model parameterization. In an attempt to accomplish this we introduce a fine discretization of the model, and hence the number of cells is large, especially in three-dimensional models. Using (4) and numerical approximations to derivatives allows the objective function in (3) to be written as

$$\begin{aligned} \phi_m(\mathbf{m}) = (\mathbf{m} - \mathbf{m}_0)^T \{ & \alpha_s \mathbf{W}_s^T \mathbf{W}_s + \alpha_x \mathbf{W}_x^T \mathbf{W}_x + \alpha_y \mathbf{W}_y^T \mathbf{W}_y \\ & + \alpha_z \mathbf{W}_z^T \mathbf{W}_z \} (\mathbf{m} - \mathbf{m}_0) \end{aligned} \quad (5)$$

where  $\mathbf{m}, \mathbf{m}_0 \in R^M$  and  $\mathbf{W}_s, \mathbf{W}_x, \mathbf{W}_y,$  and  $\mathbf{W}_z$  are  $M \times M$  matrices. Equation (5) can be written generically as

$$\phi_m(\mathbf{m}) = (\mathbf{m} - \mathbf{m}_0)^T \mathbf{W}_m^T \mathbf{W}_m (\mathbf{m} - \mathbf{m}_0) = \|\mathbf{W}_m (\mathbf{m} - \mathbf{m}_0)\|^2. \quad (6)$$

We will use this form for most derivations even though  $\mathbf{W}_m$  may not be explicitly computed. There is no loss of generality in doing this because our final computations require only  $\mathbf{W}_m^T \mathbf{W}_m$  and this is easily evaluated from (5).

With the same model parameterization, the forward mapping is written as  $\mathbf{d} = \mathcal{F}[\mathbf{m}]$  where  $\mathbf{d} \in R^N$ . The inverse problem is now formulated as the optimization problem: Minimize

$$\phi_m = \|\mathbf{W}_m (\mathbf{m} - \mathbf{m}_0)\|^2$$

subject to

$$\phi_d = \|\mathbf{W}_d (\mathbf{d} - \mathbf{d}^{\text{obs}})\|^2 = \phi_d^* \quad (7)$$

where  $\phi_d$  denotes a misfit criterion,  $\mathbf{W}_d$  is an  $N \times N$  data-weighting matrix, and  $\phi_d^*$  is the target misfit value. If the noise contaminating the  $j$ th observation is an uncorrelated Gaussian random variable having zero mean and standard deviation  $\varepsilon_j$ , then an appropriate form for  $\mathbf{W}_d$  is  $\mathbf{W}_d = \text{diag} \{1/\varepsilon_1, \dots, 1/\varepsilon_N\}$ . With this assumption,  $\phi_d$  is a random variable distributed as chi-square with  $N$  degrees of freedom. The expected value of  $\phi_d$  is therefore approximately equal to  $N$  and, accordingly, the

model sought from the inversion algorithm should reproduce the observations to about this value.

The optimization in (7) is solved by finding an  $\mathbf{m}$  and a Lagrange multiplier  $\mu$  such that the objective function

$$\phi(\mathbf{m}) = \phi_m(\mathbf{m}) + \mu^{-1}(\phi_d(\mathbf{d}) - \phi_d^*) \quad (8)$$

is minimized. (For notational convenience we use  $\mu^{-1}$  but will refer to  $\mu$  as the Lagrange multiplier.) The problem is nonlinear, so iteration is required. Let  $\mathbf{m}^{(n)}$  be the model at the  $n$ th iteration, and let  $\mathbf{d}^{(n)}$  denote the predicted data. We search for a perturbation  $\delta\mathbf{m}$  which reduces (8). Performing a first-order Taylor expansion of the data about  $\mathbf{m}^{(n)}$  yields

$$\mathbf{d}(\mathbf{m}^{(n)} + \delta\mathbf{m}) = \mathbf{d}^{(n)} + \mathbf{J}\delta\mathbf{m} \quad (9)$$

where the  $N \times M$  sensitivity matrix  $\mathbf{J}$  has elements

$$J_{ij} = \frac{\partial d_i}{\partial m_j} \quad (10)$$

The perturbed objective function is

$$\begin{aligned} \phi(\mathbf{m}^{(n)} + \delta\mathbf{m}) = & \|\mathbf{W}_m (\mathbf{m}^{(n)} + \delta\mathbf{m} - \mathbf{m}_0)\|^2 \\ & + \mu^{-1} \{ \|\mathbf{W}_d (\mathbf{d}^{(n)} + \mathbf{J}\delta\mathbf{m} - \mathbf{d}^{\text{obs}})\|^2 - \phi_d^* \} \end{aligned} \quad (11)$$

Differentiating with respect to the parameters  $\delta\mathbf{m}$  and setting the resultant equations to zero yields

$$\mathbf{B}\delta\mathbf{m} = \mathbf{b} \quad (12)$$

where

$$\mathbf{B} = \mu \mathbf{W}_m^T \mathbf{W}_m + \mathbf{J}^T \mathbf{W}_d^T \mathbf{W}_d \mathbf{J}$$

$$\mathbf{b} = -\mu \mathbf{W}_m^T \mathbf{W}_m (\mathbf{m}^{(n)} - \mathbf{m}_0) - \mathbf{J}^T \mathbf{W}_d^T \mathbf{W}_d (\mathbf{d}^{(n)} - \mathbf{d}^{\text{obs}})$$

Differentiating with respect to the Lagrange multiplier requires that

$$\|\mathbf{W}_d (\mathbf{d}^{(n)} + \mathbf{J}\delta\mathbf{m} - \mathbf{d}^{\text{obs}})\|^2 = \phi_d^* \quad (13)$$

The value of  $\mu$  may be found by simultaneously solving (12) and (13); this assumes that the linearized estimate of the misfit is an adequate approximation to the true misfit. Alternatively,  $\mu$  may be found by requiring

$$\|\mathbf{W}_d (\mathbf{d} - \mathbf{d}^{\text{obs}})\|^2 = \|\mathbf{W}_d [\mathcal{F}(\mathbf{m}^{(n)} + \delta\mathbf{m}) - \mathbf{d}^{\text{obs}}]\|^2 = \phi_d^* \quad (14)$$

Either approach requires a line search. This is an important aspect of the inversion, but discussion is postponed until later. The iterative process is continued until convergence is reached. That is, a model is found which produces a misfit equal to the target value and the model objective function undergoes no further decrease with successive iterations. This does not guarantee that a global minimum has been found.

Many inverse practitioners still consider the primary goal of the inverse problem to be that of finding a model which fits the data. The ill-posedness of the inverse problem is recognized, and some form of regularization is incorporated. Often, however, too little attention is paid to the explicit form of the regularization. The inherent nonuniqueness is generally so large that the first step in solving any inverse problem should be to design the model objective function. The objective function should be such that it produces a model with characteristics that are in accordance with the general Earth structure, is consistent with a priori information about the model, and is interpretable. The objective function in (3) has the flexibility to accomplish this. To emphasize this philosophy, we consider the inversion of an EM data set with different model objective functions.

In this paper a formalism and specific equations are presented to invert general types of EM data. However, to illustrate each of the techniques we revert to a time invariant problem, that of inverting dc resistivity data. One reason for this choice is that the dc fields are similar to fields obtained in low-frequency electromagnetic surveys, and insight about the inversion algorithms obtained by inverting dc resistivity data can be applied to frequency domain problems. Another reason is that dc inversion is made tractable because of efficient forward modeling in two and three dimensions [e.g., *Lee, 1975; Hohmann, 1975; Dey and Morrison, 1979a, b*]. This has spawned a variety of inverse solutions for the dc resistivity problem. In addition to work presented here, the interested reader is referred to *Pelton et al. [1978], Tripp et al. [1984], Smith and Vozoff [1984], Sasaki [1989], and Ramirez et al. [1993]* for examples of two-dimensional inversions and to *Park and Van [1991]* for a three-dimensional inversion.

The governing equation for dc resistivity is obtained by letting  $\omega = 0$  in (1). Setting  $M_s = 0$  yields  $\nabla \times \mathbf{E} = \mathbf{0}$  from which it follows that  $\mathbf{E} = -\nabla\Omega$

where  $\Omega$  is the electric scalar potential. Taking the divergence of the  $\mathbf{H}$  field equation yields

$$\nabla \cdot (\sigma \nabla \Omega) = \nabla \cdot \mathbf{J}_s \quad (15)$$

We may use (15) directly or, if a current of strength  $I$  is input at  $\mathbf{r}_s$  then  $\nabla \cdot \mathbf{J}_s = -I\delta(\mathbf{r} - \mathbf{r}_s)$  and (15) becomes

$$\nabla \cdot (\sigma \nabla \Omega) = -I\delta(\mathbf{r} - \mathbf{r}_s) \quad (16)$$

The boundary conditions for the potential are  $\partial\Omega/\partial n = 0$  at the Earth's surface and  $\Omega \rightarrow 0$  as  $|\mathbf{r} - \mathbf{r}_s| \rightarrow \infty$ .

In a dc survey an electric current is input to the ground, and the electric potential is measured away from the source. In the field, four electrodes are used. Two are connected to the current generator to provide a closed circuit for the current and two electrodes are needed for measuring a potential difference. However, because of superposition we can consider a pole-pole experiment in which one of the current electrodes and one of the potential electrodes are move to "infinity." This geometry can be well approximated in field acquisition and can be modeled theoretically by (16). These are the data which will be inverted in this paper.

To illustrate nonuniqueness we consider the two-dimensional conductivity structure shown in Plate 1a. It consists of a surface layer with variable conductivity, a wedge of low-conductivity material at the bottom left, and a centrally located conductive prism. The model, consisting of 1296 cells, has been slightly smoothed to make it less artificial. The geophysical survey is carried out by placing surface electrodes every 10 m in the interval  $x = (-100 \text{ m}, 100 \text{ m})$ . Each of the 21 electrode positions can be activated as a current site, and when it is, electric potentials are recorded at the remaining electrodes. The forward modeling is carried out using a finite difference algorithm [*McGillivray, 1992*]. Each of the 420 data is contaminated with Gaussian noise having a standard deviation of 5% of the datum value.

The goal of the inverse problem is to recover estimates of 1296 parameters from the inaccurate data. Four conductivity solutions, obtained after altering the coefficients  $\alpha_s$ ,  $\alpha_x$ , and  $\alpha_z$  in the generic objective function in (3), are presented in Plate 1. Each model reproduces the data to the expected value of 420. The differences in the models arise because the respective objective functions penalize

closeness to a background, vertical roughness, horizontal roughness, and roughness in both directions. All four models indicate a surface layer which is more conductive on the left than on the right. They also indicate a conductive region at depth. This provides some confidence that lateral surface variation and a zone of high conductivity at depth might be features of all models which reproduce the data. The model in Plate 1b most closely resembles the true model in Plate 1a. That is because the true model has small vertical and horizontal structure, and an objective function which penalizes roughness in both dimensions therefore produces a model with correct characteristics. It should be noted, however, that the Earth does not always act in this manner, and in some circumstances it may be that one of the other models in Plate 1 is a more realistic representation of Earth structure.

Experience has shown that the nonuniqueness exhibited in Plate 1 likely exists in EM problems in general. The degree of nonuniqueness is enlarged by measuring model length with different norms. Comparison of the effect of minimizing the  $l_1$  and  $l_2$  norms when inverting magnetotelluric data to recover one- and two-dimensional conductivity models can be found, respectively, in the works by *Whittall and Oldenburg [1992]* and *Oldenburg and Ellis [1993]*.

Having recognized the nonuniqueness inherent in electromagnetic inverse problems, we proceed to solve an EM inverse problem in which a specific objective function is minimized. The technique is essentially a Gauss-Newton method, but a subspace algorithm is used to reduce the computations required to invert the large matrix.

### 3. Subspace Algorithm

For certain problems, exact or approximate sensitivities can be efficiently calculated, and the principal roadblock is the solution of the large linear system of equations exemplified by (12). The matrix system can be solved by conjugate gradient [*Hestenes, 1980*], biconjugate gradient [*Press et al., 1992*], or LSQR [*Paige and Saunders, 1982*] and other iterative algorithms. Our approach is to use the generalized subspace method of *Oldenburg et al. [1993]*. That algorithm, and its further exploration in solving linear inverse problems [*Oldenburg and Li, 1994*], have been successfully used to invert a number of different data sets. In fact, the results

shown in Plate 1 were carried out with the subspace approach, and only a  $25 \times 25$  matrix was inverted even though estimates of 1296 parameters were obtained.

Let  $\mathbf{m}^{(n)}$  be the model at the  $n$ th iteration and let  $\{\mathbf{v}_i\}$  ( $i = 1, q$ ) be arbitrary vectors which form a  $q$ -dimensional subspace of  $R^M$ . We seek a model perturbation of the form  $\delta\mathbf{m} = \sum \alpha_i \mathbf{v}_i = \mathbf{V}\alpha$ . Substituting into (11) yields

$$\begin{aligned} \phi(\alpha) = & \|\mathbf{W}_m(\mathbf{m}^{(n)} + \mathbf{V}\alpha - \mathbf{m}_0)\|^2 \\ & + \mu^{-1}(\|\mathbf{W}_d(\mathbf{d}^{(n)} + \mathbf{J}\mathbf{V}\alpha - \mathbf{d}^{\text{obs}})\|^2 - \phi_d^*) \end{aligned} \quad (17)$$

Setting  $\nabla_\alpha \phi(\alpha) = 0$  yields

$$\mathbf{B}\alpha = \mathbf{b} \quad (18)$$

where

$$\mathbf{B} = \mathbf{V}^T(\mathbf{J}^T\mathbf{W}_d^T\mathbf{W}_d\mathbf{J} + \mu\mathbf{W}_m^T\mathbf{W}_m)\mathbf{V}$$

$$\mathbf{b} = -\mu\mathbf{V}^T\mathbf{W}_m^T\mathbf{W}_m(\mathbf{m}^{(n)} - \mathbf{m}_0) - \mathbf{V}^T\mathbf{J}^T\mathbf{W}_d^T\mathbf{W}_d(\mathbf{d}^{(n)} - \mathbf{d}^{\text{obs}})$$

The matrix  $\mathbf{B}$  is  $q \times q$ , positive definite, and symmetric and is easily inverted provided that  $q$  is relatively small. We note that this is the same matrix as in (12) except it has been contracted with the matrix  $\mathbf{V}$ .

The principal advantage of a subspace approach is that only a  $q \times q$  matrix needs to be inverted. An immediate disadvantage is that in restricting the activated portion of model space, it may be that vectors which are important in finding the global minimum of the desired objective function are not available and an inferior solution is obtained. The success or failure of a subspace approach therefore hinges upon the selection of the spanning vectors for the activated subspace. The philosophy for selecting vectors is based upon the following ideas. The two objective functions of importance to the inversion are  $\phi_m$  and  $\phi_d$ . Steepest descent vectors associated with each of these quantities are therefore fundamental to the inversion.

The misfit objective function  $\phi_d = (\mathbf{d} - \mathbf{d}_0)^T \mathbf{W}_d^T \mathbf{W}_d (\mathbf{d} - \mathbf{d}_0)$  may be partitioned as

$$\phi_d = \sum \phi_d^k \quad (19)$$

where the  $k$ th subset is  $\phi_d^k = (\mathbf{d}^k - \mathbf{d}_0^k)^T \mathbf{W}_d^{kT} \mathbf{W}_d^k (\mathbf{d}^k - \mathbf{d}_0^k)$ . The gradient  $\nabla_m \phi_d^k$  can be calculated. Our norm on model space is controlled by the symmetric positive definite matrix  $\mathbf{W}_m^T \mathbf{W}_m$ . A

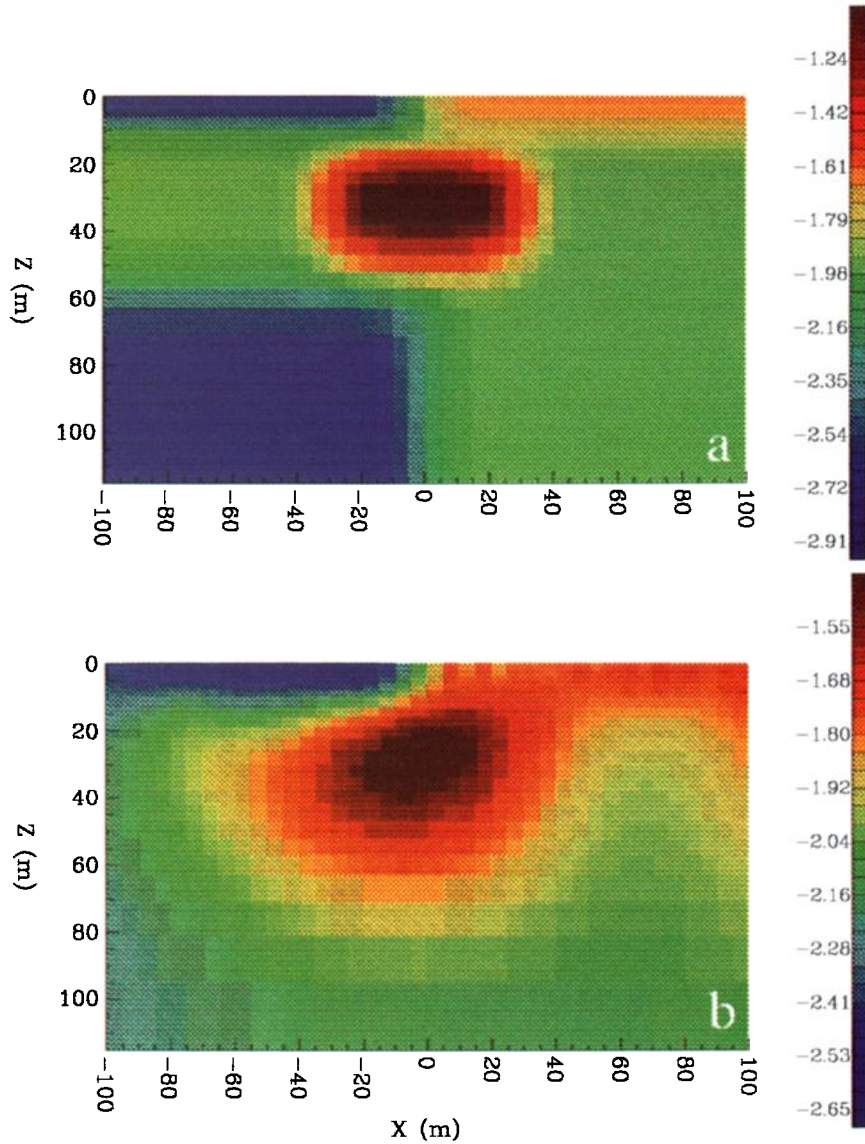


**Plate 1.** (a) The true two-dimensional conductivity structure. (b–e) Recovered model from inversion of 420 pole-pole dc resistivity data contaminated with 5% Gaussian noise fit to the expected misfit. The difference between the models results because of choices for  $\alpha_s$ ,  $\alpha_x$ , and  $\alpha_z$  which are, respectively, the weightings for “closeness” to the half-space reference model, variation in the  $x$  direction, and variation in the  $z$  direction. The values of  $(\alpha_s, \alpha_x, \alpha_z)$  for the inversions in Plate 1b–1e are respectively (0.0002, 1., 1.), (0.0002, 0., 0.), (0., 1., 0.), and (0., 0., 1.0).

steepest descent (really ascent, but we are interested only in directions and therefore ignore the minus sign) direction can be obtained by multiplying the gradient by  $(\mathbf{W}_m^T \mathbf{W}_m)^{-1}$  [Gill *et al.*, 1981, p. 102]. We therefore choose vectors

$$\mathbf{v}_k = (\mathbf{W}_m^T \mathbf{W}_m)^{-1} \nabla_m \phi_d^k \quad (20)$$

as elements in our subspace. The partitioning of  $\phi_d$  can be effected in a variety of ways, and the reader is referred to the papers cited above for further discussion and examples.

The next set of vectors to be included in the subspace should be sensitive to  $\phi_m$ . The steepest descent vector  $\mathbf{v} = (\mathbf{W}_m^T \mathbf{W}_m)^{-1} \nabla_m \phi_m$  is always

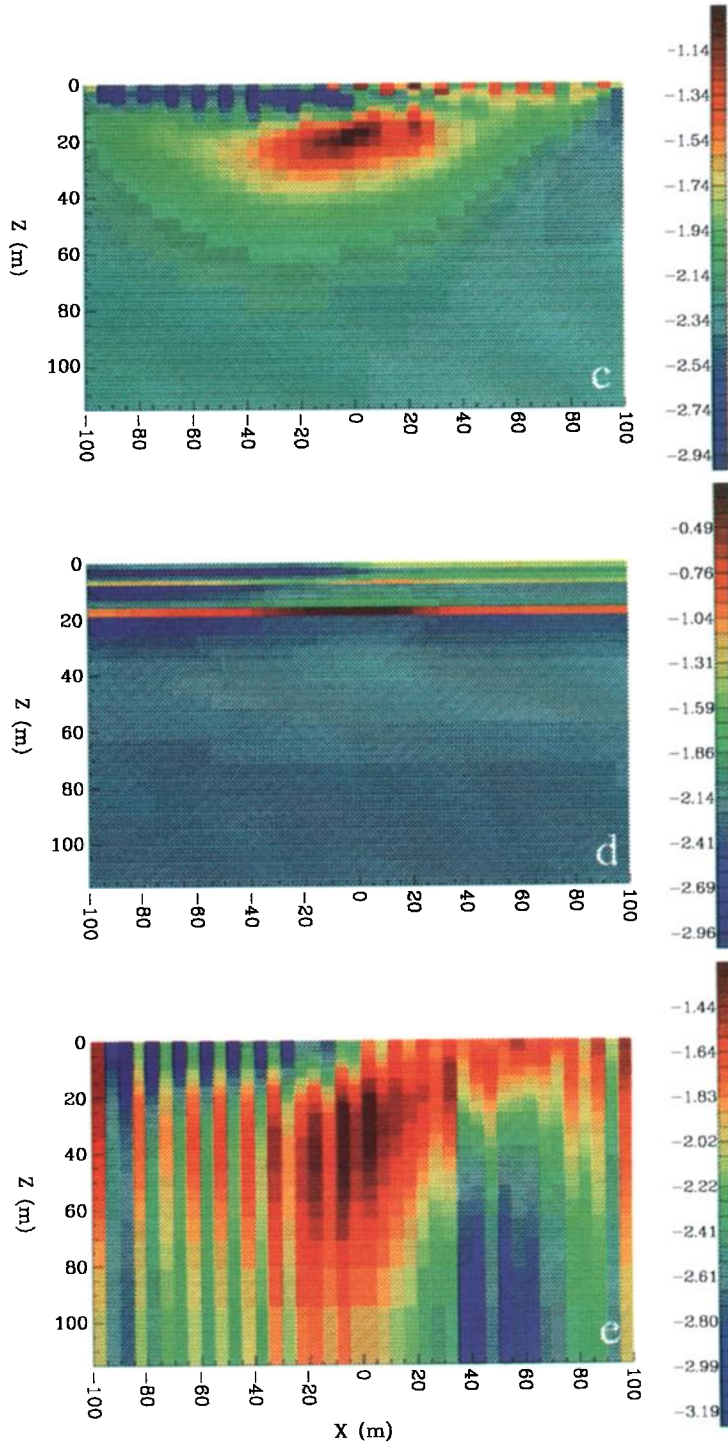


Plate 1. (continued)

useful, but more flexibility to construct a minimum norm model is achieved by subdividing the model objective function. Let  $\phi_m^k$  ( $k = 1, 4$ ) denote the  $k$ th term in the model objective function in (3). Steepest descent vectors

$$\mathbf{v}_k = (\mathbf{W}_m^T \mathbf{W}_m)^{-1} \nabla_m \phi_m^k \quad k = 1, 4 \quad (21)$$

are routinely used in our algorithm. In addition, we use the constant vector. The sum of the vectors in (21) is equal to the steepest descent vector for  $\nabla_m \phi_m$ , and potentially useful vectors can also be obtained by partitioning this. For two-dimensional problems the cells along individual rows or individual columns can be grouped, and the projection of  $(\mathbf{W}_m^T \mathbf{W}_m)^{-1} \nabla_m \phi_m$  onto those rows or columns provides good search directions, especially if the Earth model has strong lateral or vertical continuity. The analogous situation in three dimensions is to use horizontal or vertical planes of cells.

There is no definitive way to prescribe an optimum strategy for subdividing  $\nabla_m \phi_m$  or for specifying additional vectors. The process can be dynamic in that it changes with iteration. For instance, cells associated with rows could be used at one iteration, and cells associated with columns used on the next. The process can also be interactive. Viewing the model can prompt the hypothesis that a certain portion of the model has too much roughness or has other undesirable characteristics. This area can be subdivided into smaller groups of cells to provide additional flexibility in the inversion. The attractive aspect of the dynamic use of additional search vectors is that in the subspace inversion only a model perturbation is sought. At worst, a poor choice of additional vectors produces little benefit.

For each problem there may be additional vectors, inspired by insight about the character of the model, which are useful. In the most basic strategy, however, and that which is employed in the examples in this paper, we use the vectors given by (20) and (21) and the constant vector.

The inversions in Plate 1 were carried out with the following methodology. There were 21 vectors associated with data groupings (one vector for each current electrode), three vectors associated with the individual components of the model objective function, and the constant vector. In defining the model objective function (5),  $\mathbf{W}_s$  is a diagonal matrix with elements  $(\Delta x \Delta z)^{1/2}$  where  $\Delta x$  is the length of the cell and  $\Delta z$  is its thickness,  $\mathbf{W}_x$  has

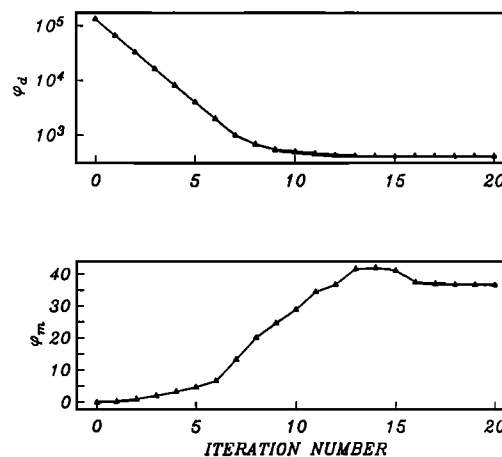


**Figure 1.** (top) The data misfit as a function of iteration. The desired misfit of 420 is achieved at iteration 13. (bottom) The model objective function curve. Convergence of the algorithm is achieved when  $\phi_d = 420$  (the target value of misfit), and no substantial reduction in the value of  $\phi_m$  is achieved with successive iterations.

elements  $\pm(\Delta z/dx)^{1/2}$  where  $dx$  is the distance between the centers of horizontally adjacent cells, and  $\mathbf{W}_z$  has elements  $\pm(\Delta x/dz)^{1/2}$  where  $dz$  is the distance between the centers of vertically adjacent cells.  $\mathbf{W}_y$  and  $\alpha_y$  are omitted since this is a two-dimensional problem. For the inversions in Plate 1b,  $\alpha_s = 0.0002$ ,  $\alpha_x = 1.0$ , and  $\alpha_z = 1.0$ . The starting and reference models are half-spaces of 5 mS/m. At each iteration a model perturbation was sought which reduced the misfit by a factor of 2 until the final target misfit was reached. The Lagrange multiplier was found with the aid of a line search using a forward modeling algorithm to evaluate (14). The convergence curves for the inversion in Plate 1b are shown in Figure 1. These are typical for the subspace algorithm.

For this problem the major computation was in generating the sensitivity matrix and forward modeling to compute observed responses and to carry out the line search. The cost of the matrix inversion was minimal, since only a  $25 \times 25$  matrix was inverted.

In addition to the selection of the search vectors there are other practical issues to be addressed in the subspace methodology. These include guarding against poor conditioning of the matrix  $\mathbf{V}$ , selection of the Lagrange multiplier at each iteration, and guarding against a poor perturbation.

The subspace formulation demands the inversion

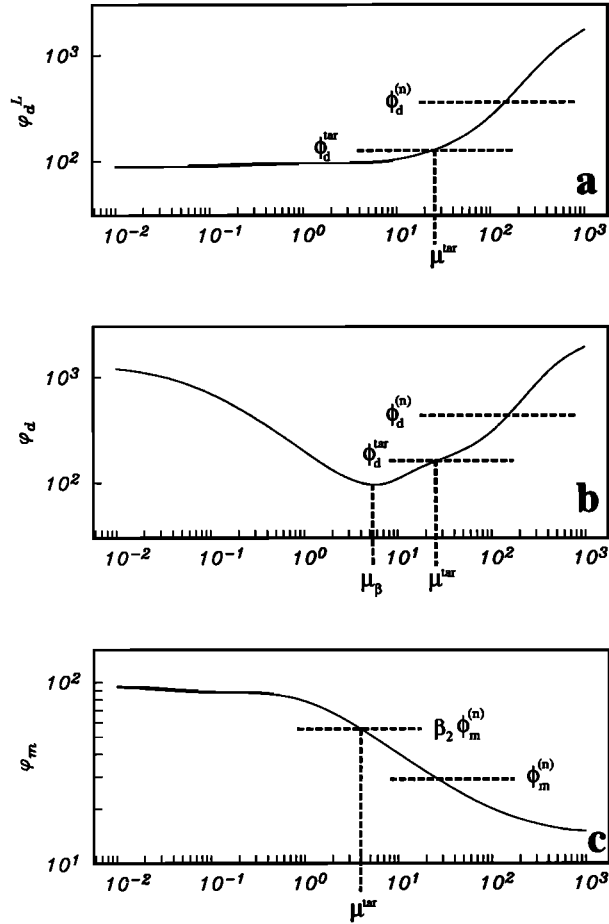


**Figure 2.** Curves used to estimate the Lagrange multiplier at each iteration, showing typical plots of (a) the linearized misfit ( $\phi_d^L$ ), (b) the nonlinear misfit ( $\phi_d$ ) which is evaluated using forward modeling, and (c) the value of the model norm ( $\phi_m$ ). The variables  $\phi_d^{(n)}$  and  $\phi_m^{(n)}$  are the data misfit and the value of the model objective function at the end of the  $n$ th iteration, and  $\phi_d^{\text{tar}}$  is the desired misfit for the current iteration.

of the matrix  $\mathbf{V}^T(\mathbf{J}^T\mathbf{W}_d^T\mathbf{W}_d\mathbf{J} + \mu\mathbf{W}_m^T\mathbf{W}_m)\mathbf{V}$ . This matrix is singular if the column vectors of  $\mathbf{V}$  are linearly dependent. Poor conditioning is avoided by orthonormalizing the descent vectors prior to using them in the subspace equations.

The solution of the matrix system in (18) is attacked in the following manner. At each iteration the trade-off between the Lagrange multiplier, the model objective function, and the misfit is typified by the curves in Figure 2. Figure 2a characterizes the linearized estimate of misfit and is obtained by

specifying a value for  $\mu$ , solving (18), and computing

$$\phi_d^L = \|\mathbf{W}_d(\mathbf{d}^{(n)} + \mathbf{J}\mathbf{V}\alpha - \mathbf{d}^{\text{obs}})\|^2 \quad (22)$$

This is easily computed, since it requires only repetitive solution of a  $q \times q$  system of equations with trial values of  $\mu$ . Let the target misfit for each iteration be denoted by  $\phi_d^{\text{tar}} = \beta_1 \phi_d^{(n)}$ . If the target can be reached with a small change in the model, then the estimation of  $\mu$  using Figure 2a may provide an acceptable step. This is often valid at early and late iterations in the inversion. When the model perturbation is large, however, the linearized misfit is not acceptably close to the true misfit defined by (14). Under such circumstances,  $\mu$  should be estimated from Figure 2b. This requires more computation, since generating each point on this curve requires that a forward modeling be carried out. If  $\phi_d^{\text{tar}}$  lies above the minimum of the misfit curve, then  $\mu^{\text{tar}}$  is the estimated value of the Lagrange multiplier, while if  $\phi_d^{\text{tar}}$  lies below, then  $\mu_B$  is selected. The curve in Figure 2c is used to limit the increase in the model objective function at any iteration. This is of practical importance. Misfit can often be reduced quickly but at the expense of producing a model with undesirable structure. Once the target misfit has been reached, numerous iterations may be required to remove those features and bring  $\phi_m$  to its minimum value. A strategy which limits the rate of increase of  $\phi_m$  may take more iterations to reach the target misfit but ultimately requires fewer iterations for convergence. Let  $\mu^{\text{mod}}$  be that value of  $\mu$  such that the model objective function is equal to  $\beta_2 \phi_m^{(n)}$ . Irrespective of whether  $\phi_d^L(\mu)$  or  $\phi_d(\mu)$  is used, the chosen value of  $\mu$  is given by  $\mu = \max\{\mu^{\text{tar}}, \mu^{\text{mod}}\}$ . If  $\mu^{\text{tar}}$  does not exist for the nonlinear misfit, then  $\mu^{\text{tar}}$  is replaced by  $\mu_B$ .

For simplicity, in the subspace solution carried out here we evaluated the misfit according to (14) for all iterations. We set  $\beta_1$  to 0.5, and  $\beta_2 = 2.0$  once a misfit within a factor of 10 of the final target misfit was achieved. Typically, four forward modelings per iteration were needed in our line search to estimate  $\mu^{\text{tar}}$  or  $\mu_B$ .

#### 4. Calculation of Sensitivities for Frequency Domain EM Problems

An essential element in almost all formulations of the inverse problem is the ability to compute the numerical sensitivities. General procedures exist

for doing this (e.g., see *McGillivray and Oldenburg* [1990] for a review of commonly used methods and an introduction to relevant literature). For inverse problems having more unknowns than data, it is advantageous to use an adjoint equation or Green's function approach. Formal derivations exist [e.g., *Lanczos*, 1961; *Morse and Feshbach*, 1953; *Roach*, 1982], and their application to electromagnetic induction problems has been presented by *Weidelt* [1975], *Park* [1987], *Madden and Mackie* [1989], *Madden* [1990], *Oldenburg* [1990], and *Ellis and Oldenburg* [1994a], as well as others. The usual procedure for implementation requires the development of an adjoint operator which is formulated through the use of the bilinear identity. That identity also establishes the reciprocity condition for EM data which is needed so that the sensitivity computations can be carried out efficiently. A simplified derivation which leads to the same equations as the adjoint formulation is presented by *McGillivray et al.* [1994]. The work here is based upon that derivation.

Our goal is to compute the sensitivity  $J_{ik} = \partial d_i / \partial \sigma_k$  where  $d_i$  is the  $i$ th datum and  $\sigma_k$  is the conductivity of the  $k$ th cell. The datum  $d_i$  may take many forms; it could be an admittance, an impedance, a component of  $\mathbf{E}$  or  $\mathbf{H}$ , an amplitude, or a phase. Irrespective of the choice of  $d_i$ , the basic building block for computing  $J_{ik}$  is the ability to compute  $\partial \mathbf{E} / \partial \sigma_k$  and  $\partial \mathbf{H} / \partial \sigma_k$ . If the inversion parameters are  $m_k = \ln \sigma_k$  instead of  $\sigma_k$ , then appropriate sensitivities are generated by  $\partial \mathbf{E} / \partial \ln \sigma_k = \sigma_k \partial \mathbf{E} / \partial \sigma_k$ .

Substituting  $\sigma(\mathbf{r}) = \sum \sigma_k \psi_k(\mathbf{r})$  into (1) and differentiating with respect to  $\sigma_k$  produces the sensitivity equations,

$$\nabla \times \frac{\partial \mathbf{E}}{\partial \sigma_k} = -i\omega\mu \frac{\partial \mathbf{H}}{\partial \sigma_k} \quad (23)$$

$$\nabla \times \frac{\partial \mathbf{H}}{\partial \sigma_k} = (\sigma + i\omega\epsilon) \frac{\partial \mathbf{E}}{\partial \sigma_k} + \psi_k(\mathbf{r})\mathbf{E}$$

and homogenous boundary conditions of the form

$$\alpha \left( \hat{\mathbf{n}} \times \frac{\partial \mathbf{U}}{\partial \sigma_k} \right) + \beta \left( \hat{\mathbf{n}} \times \hat{\mathbf{n}} \times \nabla \times \frac{\partial \mathbf{U}}{\partial \sigma_k} \right) = \mathbf{0}. \quad (24)$$

Next consider an auxiliary Maxwell problem,

$$\nabla \times \tilde{\mathbf{E}} = -i\omega\mu \tilde{\mathbf{H}} + \tilde{\mathbf{M}}_s \quad (25)$$

$$\nabla \times \tilde{\mathbf{H}} = (\sigma + i\omega\epsilon) \tilde{\mathbf{E}} + \tilde{\mathbf{J}}_s$$

where the electric and magnetic sources  $\tilde{\mathbf{J}}_s$  and  $\tilde{\mathbf{M}}_s$  have yet to be defined. The boundary value problem can be solved once the conditions appropriate to  $\tilde{\mathbf{J}}_s$  and  $\tilde{\mathbf{M}}_s$  are specified on  $\partial D$ . These have the form

$$\tilde{\alpha}(\hat{\mathbf{n}} \times \tilde{\mathbf{U}}) + \tilde{\beta}(\hat{\mathbf{n}} \times \hat{\mathbf{n}} \times \nabla \times \tilde{\mathbf{U}}) = \mathbf{0} \quad (26)$$

We note that these boundary conditions may differ from those used to solve the primal problem in (1). For instance, the primal problem might be a magnetotelluric problem whose source is a sheet of current at height, but the source for the auxiliary problem is likely a current or magnetic dipole inside  $\partial D$ . With the exception of the changes in the specifics of the boundary conditions and practical details regarding meshing of the domain, the solution of the forward and auxiliary problems can likely be obtained by using the same computing algorithm.

Combining (23) and (25) and manipulating yields the result

$$\int_D \left( \tilde{\mathbf{M}}_s \cdot \frac{\partial \mathbf{H}}{\partial \sigma_k} + \tilde{\mathbf{J}}_s \cdot \frac{\partial \mathbf{E}}{\partial \sigma_k} \right) dv = \int_D \tilde{\mathbf{E}} \cdot \mathbf{E} \psi_k(\mathbf{r}) dv \quad (27)$$

This shows that the sensitivity for  $\mathbf{E}$  or  $\mathbf{H}$  can be obtained by appropriately specifying the sources for the auxiliary fields and by integrating the dot product of the primal and auxiliary electric fields over the region on which  $\psi_k(\mathbf{r})$  is nonzero. For example, to obtain the sensitivities for  $H_z$  at an observation location  $\mathbf{r}_0$ , let  $\tilde{\mathbf{M}}_s = \delta(\mathbf{r} - \mathbf{r}_0)\hat{\mathbf{z}}$  and  $\tilde{\mathbf{J}}_s = \mathbf{0}$ . Then (27) becomes

$$\frac{\partial H_z(\mathbf{r}_0)}{\partial \sigma_k} = \int_D \tilde{\mathbf{E}} \cdot \mathbf{E} \psi_k(\mathbf{r}) dv. \quad (28)$$

The primal problem is solved for the electric field  $\mathbf{E}$ , and the auxiliary problem, with a unit vertical magnetic dipole source placed at  $\mathbf{r}_0$ , is solved for the auxiliary electric field  $\tilde{\mathbf{E}}$ . The quantity  $\tilde{\mathbf{E}} \cdot \mathbf{E}$  is integrated to generate  $\partial H_z / \partial \sigma_k$ .

The sensitivity equation for the dc resistivity problem is directly derivable from (27). Setting  $\tilde{\mathbf{M}}_s = \mathbf{0}$  and using standard vector identities we have

$$\int \tilde{\mathbf{J}}_s \cdot \frac{\partial \mathbf{E}}{\partial \sigma_k} dv = - \int \left[ \nabla \cdot \left( \tilde{\mathbf{J}}_s \frac{\partial \Omega}{\partial \sigma_k} \right) - \frac{\partial \Omega}{\partial \sigma_k} \nabla \cdot \tilde{\mathbf{J}}_s \right] dv \quad (29)$$

Applying Gauss's theorem to the first term and using the fact that  $\mathbf{J}_s \cdot \mathbf{n} = 0$  on the top boundary

and  $\Omega = 0$  on the other boundaries allows the sensitivity to be written as

$$\int \frac{\partial \Omega}{\partial \sigma_k} \nabla \cdot \bar{\mathbf{J}}_s \, dv = \int_D \bar{\mathbf{E}} \cdot \mathbf{E} \psi_k(\mathbf{r}) \, dv \quad (30)$$

Setting  $\nabla \cdot \bar{\mathbf{J}}_s = -I_u \delta(\mathbf{r} - \mathbf{r}_0)$  where  $I_u$  is a unit amplitude current, so that the auxiliary equation becomes

$$\nabla \cdot (\sigma \nabla \bar{\Omega}) = -I_u \delta(\mathbf{r} - \mathbf{r}_0), \quad (31)$$

and writing the electric fields in terms of their respective potentials, yields the final equations

$$\frac{\partial \Omega(\mathbf{r}_0)}{\partial \sigma_k} = - \int_D \nabla \bar{\Omega} \cdot \nabla \Omega \psi_k(\mathbf{r}) \, dv \quad (32)$$

Calculation of sensitivities via (27) for general EM problems may require numerous forward modelings, but computational efficiencies are achieved if sources and receivers occupy the same position or if the final fields from one forward modeling are used as starting fields for a next solution. We also note that (27) lends itself to the estimation of approximate sensitivities obtained by inserting an electric field that approximates that due to the auxiliary field. The paper by *Habashy et al.* [1993] and the work derived therefrom have much potential in this regard.

In the next section we are interested in computing a large-scale sensitivity or the change in the objective function with respect to a model parameter. Consider the computation of

$$\frac{\partial \phi_d}{\partial \sigma_k} = \frac{\partial}{\partial \sigma_k} \sum_{i=1}^N \left( \frac{d_i - d_i^{\text{obs}}}{\epsilon_i} \right)^2 = 2 \sum_{i=1}^N \left( \frac{d_i - d_i^{\text{obs}}}{\epsilon_i^2} \right) \frac{\partial d_i}{\partial \sigma_k}. \quad (33)$$

The linearity of Maxwell's equations with respect to applied sources means that the computation of  $\partial \phi_d / \partial \sigma_k$  is easily accomplished by generating the electric fields due to a superposition of sources of strength  $2(d_i - d_i^{\text{obs}}) / \epsilon_i^2$  located at the receiver locations. This necessitates only a single forward modeling. For the dc problem the desired electric field comes from solving the auxiliary problem

$$\nabla \cdot (\sigma \nabla \bar{\Omega}) = 2 \sum_{i=1}^N \left( \frac{d_i - d_i^{\text{obs}}}{\epsilon_i^2} \right) \delta(\mathbf{r} - \mathbf{r}_i). \quad (34)$$

## 5. Conjugate Gradient Solution

In large-scale inverse problems it may not be possible to compute and store the sensitivity matrix. The next choice of solution method is to use conjugate gradients [*Hestenes*, 1980] to minimize a nonquadratic objective functional. The steps are essentially the following. First, write the objective function (8) as  $\phi(\mathbf{m}) = \phi_d(\mathbf{m}) + \mu \phi_m(\mathbf{m})$ . The quantity  $\mu$  is now regarded as a trade-off parameter as it alters the relative weighting between the model and data misfit objective functions. Its value is supplied by the user. To minimize  $\phi(\mathbf{m})$ , an iterative method is used where the gradient of the objective function

$$\nabla_m \phi(\mathbf{m}) = \nabla_m \phi_d(\mathbf{m}) + \mu \nabla_m \phi_m(\mathbf{m}) \quad (35)$$

is formed at each iteration. In generating (35) the partial gradient  $\nabla \phi_d$  is efficiently found using the method described in section 3. A forward modeling with sources at receiver locations and with source strengths proportional to data misfit is carried out to compute the auxiliary electric field. The individual terms  $\partial \phi_d / \partial \sigma_k$  are then obtained by integrating the product of the primary and auxiliary fields over the  $k$ th cell. The gradient of the model objective function,  $2\mathbf{W}_m^T \mathbf{W}_m(\mathbf{m} - \mathbf{m}_0)$ , is found directly. The next step is to generate the steepest descent vector  $\gamma = (\mathbf{W}_m^T \mathbf{W}_m)^{-1} \nabla_m \phi(\mathbf{m})$ . Rather than finding an optimum model perturbation along the vector  $\gamma$  as in a steepest descent algorithm, a univariate search along that portion of  $\gamma$  which is conjugate to all of the previous directions is performed. Variants of the conjugate gradient (CG) algorithm exist [*Hestenes*, 1980; *Press et al.*, 1992], but the algorithm of *Polyak and Ribiere* [1969] is recommended.

1. Choose  $\mathbf{m}^{(1)}$  and set  $\mathbf{r}^{(1)} = -\gamma(\mathbf{m}^{(1)})$ ,  $\mathbf{p}^{(1)} = \mathbf{r}^{(1)}$ .

2. Choose  $\alpha = \alpha^k$  to minimize  $\phi(\alpha) = \phi(\mathbf{m}^{(k)} + \alpha \mathbf{p}^{(k)})$

$$\mathbf{m}^{(k+1)} = \mathbf{m}^{(k)} + \alpha^k \mathbf{p}^{(k)} \quad \mathbf{r}^{(k+1)} = -\gamma(\mathbf{m}^{(k+1)}) \quad (36a)$$

3. When  $k/M$  is an integer set  $\mathbf{p}^{(k+1)} = \mathbf{r}^{(k+1)}$ ; otherwise set

$$\mathbf{p}^{(k+1)} = \mathbf{r}^{(k+1)} + b^k \mathbf{p}^{(k)}, \quad b^k = \frac{|\mathbf{r}^{(k+1)}|^2 - \mathbf{r}^{(k)} \cdot \mathbf{r}^{(k+1)}}{|\mathbf{r}^{(k)}|^2} \quad (36b)$$

4. Terminate at the  $j$ th step if  $|\mathbf{r}^{(j+1)}|$  is sufficiently small.

In theory, the algorithm is reset every  $M$  iterations, where  $M$  is the number of parameters in the model. However, in practice the algorithm usually converges before the  $M$ th iteration.

For electromagnetic problems the most CPU intensive part of a conjugate gradient algorithm is forward modeling which is necessary to compute the data for a given model, the value of the objective function, and as implied in (33), the gradient of the objective function. Further, a univariate minimization must be performed at each iteration of the conjugate gradient algorithm to determine the constant  $\alpha$ .

The efficacy of the CG is illustrated by reproducing the results from a three-dimensional inversion of pole-pole dc resistivity data given by *Ellis and Oldenburg* [1994b]. The reader is referred to their paper for details of the algorithm and for further examples. The forward modeling was performed with a finite difference approximation to the physical equations, and the data and model were respectively defined as  $\ln V$  and  $\ln \sigma$ . The model objective function was a discretized form of the Sobolov-Laplacian operator,

$$\phi(m) = \int ((1 - \varepsilon)\nabla^2 m - \varepsilon m)^2 dv \quad 0 < \varepsilon \leq 1 \quad (37)$$

The test of the conjugate gradient inversion algorithm is carried out on a conductivity model consisting of five prisms and shown in Figure 3. It consists of three surface prisms (S1, S2, S3) of resistivities 200, 100, and 2000  $\Omega$  m and two buried prisms (B1, B2) of resistivities of 2000 and 100  $\Omega$  m, all in a 1000  $\Omega$  m background half-space. The surface prisms are designed to simulate near-surface conductivity variations, and the buried prisms are the survey targets. The model was discretized into  $n_x \times n_y \times n_z = 17,496$  cells where  $(n_x, n_y, n_z) = (27, 27, 24)$ .

Data were collected on a uniform square array of  $21 \times 21$  electrodes placed on a 50-m grid on the surface. The electrode array was centered on the model space shown in Figure 3. Each electrode was taken as a current electrode, and potentials were recorded from all electrodes in the electrode array within a radius of 500 m. This yielded a total of 87,688 potential data. Unbiased Gaussian noise of 1% was added to the potentials before inversion.

The starting model for the inversion was chosen to be a uniform half-space of 1000  $\Omega$  m. The

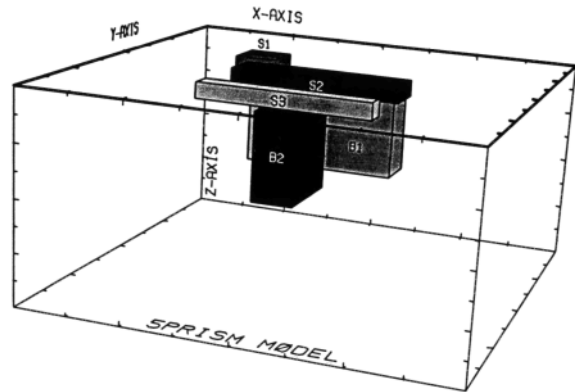


**Figure 3.** A perspective view of the five-prism model, which consists of three surface prisms S1, S2, and S3 (resistivities 200, 100, and 2000  $\Omega$  m, respectively) and two buried prisms B1 and B2 (with resistivities 2000 and 100  $\Omega$  m). The surface prisms extend from surface to a depth of 40 m, the buried prism B1 extends from depth 50 to 250 m and the buried prism B2 extends from 95 to 275 m. The resistivity of the half-space is 1000  $\Omega$  m.

inversion was run for 39 iterations to produce an rms misfit of 1%. This took a total of 97 applications of the forward modeling algorithm (including objective function gradient modeling). The value  $\varepsilon = 0.97$  was used in defining the model objective function in (37). The results of the inversion are shown in Plate 2, where three slices through the true model and the inversion result are displayed. All five blocks are well resolved, although definition of the resistive blocks is slightly poorer than for the conductive blocks. This is expected since the resistive blocks are only twice as resistive as the background whereas the contrasts between the conductive bodies and the host are 5 and 10. The convergence characteristics of the algorithm are provided in Figure 4, where the total objective function is plotted as a function of iteration. Since the appropriate value of  $\mu$  which corresponds to a particular data misfit and model roughness is not known at the beginning of the inversion, some estimate must be made. In practice, an initial value of  $\mu$  is chosen, and several iterations performed. If the convergence plot begins to plateau at an excessive misfit, then a smaller value of  $\mu$  is selected. For this example, three values  $\mu = 10^{-1}$ ,  $10^{-2}$ , and  $10^{-3}$  were used to reach an rms data misfit of 1.0%.

## 6. Approximate Inverse Mapping

As the size of the problem increases, it is not feasible to compute  $\nabla_m \phi_m$  as with the CG ap-

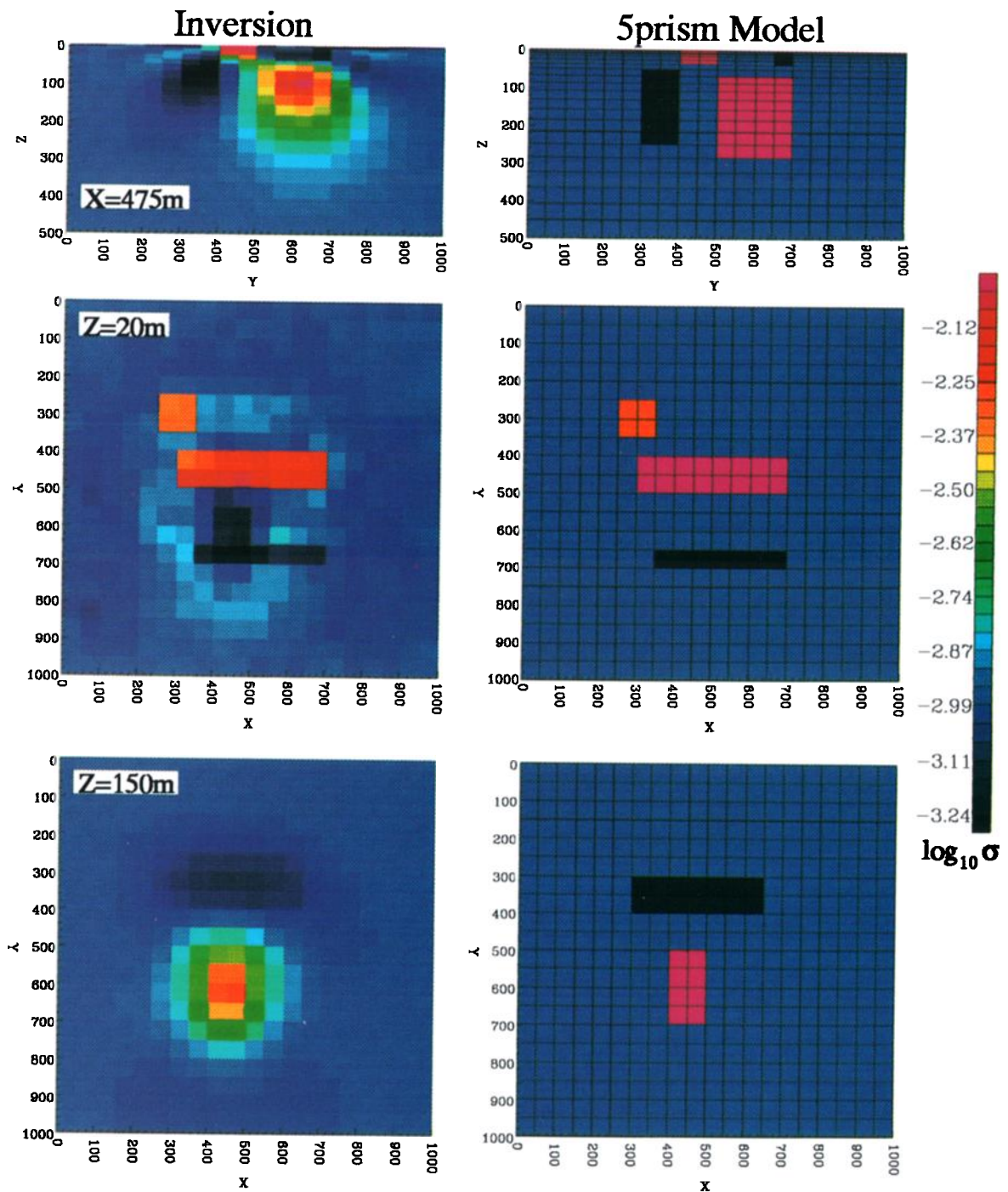


**Plate 2.** Three slices through the five-prism conductivity model (right) and the corresponding slices for the inversion result (left). (top) Vertical section through the model at  $x = 475$  m. (middle) Horizontal section at  $z = 20$  m. (bottom) Horizontal section at  $z = 150$  m. The color bar shows  $\log_{10} \sigma$  and applies to all panels.

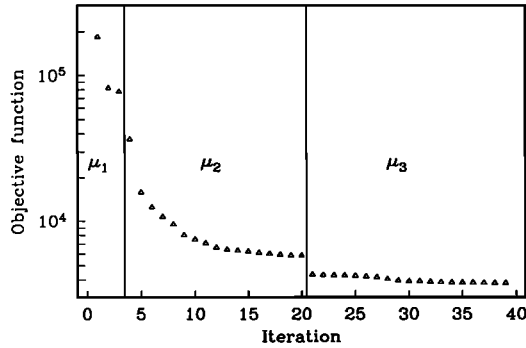


**Figure 4.** The convergence plot for the conjugate gradient inversion which produced the model shown in Plate 2. The total objective function is plotted as a function of iteration. The solid lines indicate the iterations at which the value of the trade-off parameter  $\mu$  was altered. The three values are  $\mu_1 = 10^{-1}$ ,  $\mu_2 = 10^{-2}$ , and  $\mu_3 = 10^{-3}$ . By iteration 39 the rms misfit to the data was 1% misfit.

proach, and an inversion methodology which requires only one forward modeling per iteration is required. In such cases we appeal to the approximate inverse mapping (AIM) formalism of *Oldenburg and Ellis* [1991]. The essence of the approach is presented here, but the reader is referred to the cited paper for more thorough explanation and examples.

The AIM formalism is based upon the existence of two mappings. Let  $\mathcal{F}$  be an exact forward mapping which maps an element of model space to an element of data space and let  $\tilde{\mathcal{F}}^{-1}$  be an approximate inverse mapping. Application of  $\tilde{\mathcal{F}}^{-1}$  to the data produces a model  $\tilde{\mathcal{F}}^{-1}[d^{\text{obs}}] = \tilde{m}^{\text{obs}}$ , but it is unlikely that  $\mathcal{F}[\tilde{m}^{\text{obs}}]$  acceptably reproduces the observations. With iterative improvement, however, it may be possible to use  $\tilde{\mathcal{F}}^{-1}$  to find a model which significantly reduces the misfit error.

Two procedures are possible. In AIM-MS a perturbation in model space is generated at each iteration, while in AIM-DS an alteration to the data is sought such that the application of  $\tilde{\mathcal{F}}^{-1}$  to the altered data yields a model which adequately satisfies the observations. The underlying concept of the algorithms can be understood from the schematic diagrams in Figure 5. We consider AIM-MS first. Let  $m \in \mathcal{H}_m$  be any model in a Hilbert space  $\mathcal{H}_m$ . Application of  $\mathcal{F}$  followed by an application of  $\tilde{\mathcal{F}}^{-1}$  yields an element  $\tilde{m} \in \mathcal{H}_m$ . Because the inverse mapping is approximate, it is not expected that  $\tilde{m}$  will equal  $m$ . The discrepancy is quantified by the model space mapping error

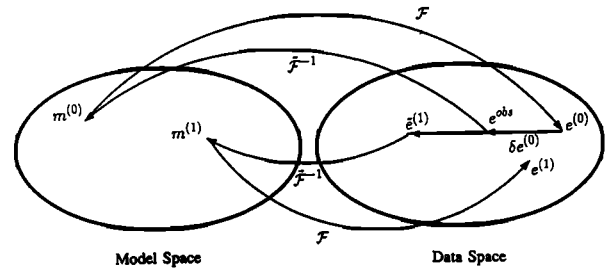
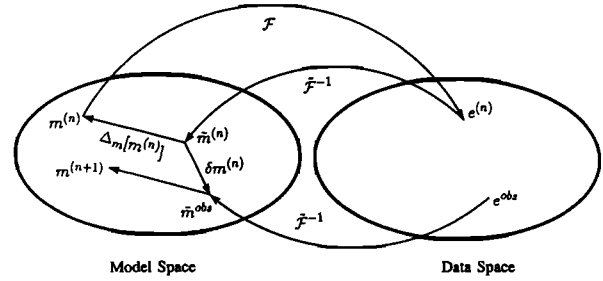


**Figure 5.** (top) A diagrammatic representation of the AIM-MS inversion. The inversion starts with  $\tilde{\mathcal{F}}^{-1}$  applied to  $d^{\text{obs}}$  to produce a first model estimate  $\tilde{m}^{\text{obs}}$ . The mapping error  $\Delta_m[m^{(n)}]$  at the current model,  $m^{(n)}$ , is used to produce the  $(n+1)$ th model. (bottom) A diagrammatic representation of the AIM-DS inversion. The inversion starts with  $\tilde{\mathcal{F}}^{-1}$  applied to  $d^{\text{obs}}$  to produce a first model estimate  $m^{(0)}$ . An exact forward mapping is applied to yield predicted data  $d^{(0)}$ . The difference between  $d^{\text{obs}}$  and  $d^{(0)}$  is an estimate of the data space mapping error. The predicted data are corrected by this difference to yield a new datum  $d^{(1)}$ . The updating of data is continued recursively.

$$\Delta_m[m] \equiv m - \tilde{\mathcal{F}}^{-1}\mathcal{F}[m] = (\mathcal{I}_m - \tilde{\mathcal{F}}^{-1}\mathcal{F})[m] = m - \tilde{m} \quad (38)$$

where  $\mathcal{I}_m$  is the identity mapping on  $\mathcal{H}_m$ . If  $m$  is a solution to the inverse problem, that is, if  $\mathcal{F}[m] = d^{\text{obs}}$ , then (38) can be written as  $m = \tilde{m}^{\text{obs}} + \Delta_m[m]$ . Since  $m$  is not known, the iterative equation

$$m^{(n+1)} = \tilde{m}^{\text{obs}} + \Delta_m[m^{(n)}] = \tilde{m}^{\text{obs}} + m^{(n)} - \tilde{m}^{(n)} \quad (39)$$

where  $\tilde{m}^{(n)} = \tilde{\mathcal{F}}^{-1}[d^{(n)}] = \mathcal{F}\tilde{\mathcal{F}}^{-1}(m^{(n)})$  is used.

Equation (39) is appealing because of its computational efficiency and also because of the intuition it conveys. It shows that the final solution is composed of two parts. The first is  $\tilde{m}^{\text{obs}}$ , which is that portion of the model recovered by applying  $\tilde{\mathcal{F}}^{-1}$  to the data. The second part of (39) is a remainder needed to account for the deficiency of  $\tilde{\mathcal{F}}^{-1}$ . We

note that  $\Delta_m = (\mathcal{F}_m - \mathcal{F}^{-1}\mathcal{F})$  has the form of a projection operator. Its application to any element of  $\mathcal{H}_m$  quantifies that part of the model which is annihilated by the approximate inverse mapping. The two terms in (39) are therefore needed to generate a model.

The goal in AIM-DS is to find a ‘‘correction’’ to the observed data so that when  $\mathcal{F}^{-1}$  is applied to the corrected data, the resultant model reproduces the observed data when it is operated upon by the exact forward mapping. That is, the inverse problem is solved by finding a data perturbation such that a new datum  $\vec{d} = d^{\text{obs}} + \xi$  satisfies  $\mathcal{F}\mathcal{F}^{-1}[\vec{d}] = d^{\text{obs}}$ . The advantage of this approach is that the desired characteristics of the final model may be built directly into  $\mathcal{F}^{-1}$  since the model is computed directly by a single application of  $\mathcal{F}^{-1}$ .

With reference to Figure 5, define a mapping error on data space as

$$\Delta_d[d] = (\mathcal{F}_d - \mathcal{F}\mathcal{F}^{-1})[d] \quad (40)$$

where  $\mathcal{F}_d$  is the identity map. Applying (40) to  $\vec{d}^{(n)}$  yields

$$\vec{d}^{(n)} = d^{(n)} - \Delta_d[\vec{d}^{(n)}]. \quad (41)$$

Setting  $d^{(n)} = d^{\text{obs}}$  yields the iterative equation

$$\vec{d}^{(n+1)} = d^{\text{obs}} + \Delta_d[\vec{d}^{(n)}] = d^{\text{obs}} + \vec{d}^{(n)} - d^{(n)} \quad (42)$$

It shows explicitly that the desired perturbation is the data space mapping error.

The AIM approach will now be used to invert pole-pole dc resistivity data to recover a three-dimensional conductivity structure. The specification of  $\mathcal{F}^{-1}$  is that given by *Li and Oldenburg* [1992] in their approximate inversion of dc resistivity data. Let the electrical conductivity in a lower half-space be  $\sigma(\mathbf{r}) = \sigma_0\mu(\mathbf{r})$  where  $\sigma_0$  is the conductivity of a uniform background and  $\mu(\mathbf{r})$  is a dimensionless function of spatial position  $\mathbf{r}$ . Under the Born approximation the relative potential anomaly defined by the ratio of the secondary to primary potential,  $\delta\Omega = \Omega_s/\Omega_p$ , measured by a pole-pole array over a flat surface is given by

$$\delta\Omega(\mathbf{r}_0, \mathbf{l}) = \int \ln \mu(\mathbf{r}) \otimes \otimes g(\mathbf{r}; \mathbf{l}) dz \quad (43)$$

where  $g(\mathbf{r}; \mathbf{l})$  is the kernel function

$$g(\mathbf{r}; \mathbf{l}) = -\frac{1}{\pi} \nabla \frac{1}{|\mathbf{r} + \mathbf{l}|} \cdot \nabla \frac{1}{|\mathbf{r} - \mathbf{l}|} \quad (44)$$

and the two circled crosses denote convolution in the  $x$  and  $y$  directions. The datum is recorded at the midpoint of an array specified by the current and potential electrodes at  $\mathbf{r}_s$  and  $\mathbf{r}_{\text{obs}}$ , respectively. The two-dimensional vector  $\mathbf{l}$  defines the relative position of the two electrodes such that  $\mathbf{r}_s - \mathbf{r}_{\text{obs}} = 2\mathbf{l}$ .

Taking the two-dimensional Fourier transform of (43) and applying the convolution theorem yields

$$\vec{f}_j(p, q) = \int_0^\infty \bar{m}(p, q, z) \bar{g}_j(p, q, z) dz \quad (45)$$

where  $(p, q)$  are the wavenumbers in the  $x$  and  $y$  directions and

$$\begin{aligned} \vec{f}_j(p, q) &= F_{xy}[\delta\Omega(\mathbf{r}_0; \mathbf{l}_j)] \quad j = 1, \dots, n_l \\ \bar{m}(p, q, z) &= F_{xy}[\ln \mu(\mathbf{r})] \end{aligned} \quad (46)$$

$$\bar{g}_j(p, q, z) = F_{xy}[g(\mathbf{r}; \mathbf{l}_j)] \quad j = 1, \dots, n_l.$$

$F_{xy}$  denotes the two-dimensional Fourier transform. The index  $j$  identifies the  $j$ th pole-pole array. If there are  $n_l$  distinct pole-pole arrays then there are  $n_l$  pole-pole maps available for Fourier transforming. This produces  $n_l$  (complex) data at each wavenumber  $(p, q)$ . Equation (45) is a Fredholm equation of the first kind, and a linear inversion can be used to recover  $\bar{m}(p, q, z)$  using the  $n_l$  complex data. The three-dimensional conductivity model in the spatial domain is then obtained by applying an inverse two-dimensional Fourier transform to  $\bar{m}$  at all depths. This process defines  $\mathcal{F}^{-1}$  as a three-dimensional inverse operator which is effected in the spatial domain by a sequence of one-dimensional inversions in the wavenumber domain. Application of this approximate inversion to data produces a conductivity output that generally displays major features of the true conductivity, but details are incorrect and usually the model does not adequately reproduce the data. An iterative AIM procedure is needed to generate a model which reproduces the data.

We consider again the synthetic data generated from the five-prism model in Figure 3. The electrodes form the same  $21 \times 21$  array with a grid spacing  $\delta = 50$  m. From this, eight pole-pole data maps are formed in both  $x$  and  $y$  directions with

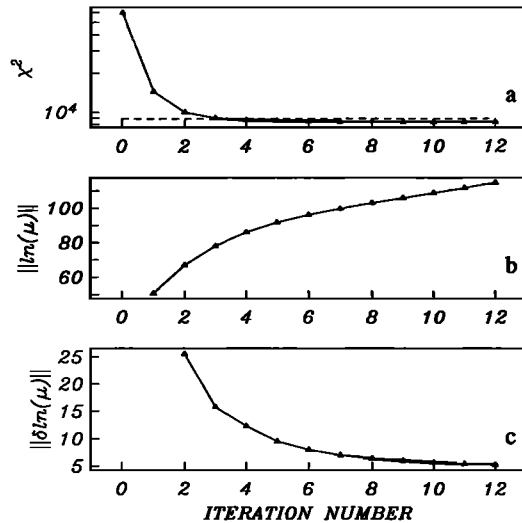


**Figure 6.** Convergence plots of the AIM-MS inversion applied to noisy data from the five-prism model. (a) Chi-square data misfit as a function of iteration. The dashed line indicates the expected misfit of 8804. This is achieved at the fourth iteration, but the algorithm has been allowed to continue so that its performance can be evaluated. (b) Model norm. (c) Norm of the model perturbation.

array separation equal to  $n\delta$  ( $n = 1, \dots, 8$ ). Five maps are also formed in  $xy$  and  $yx$  diagonal directions with separations equal to  $n\sqrt{2}\delta$  ( $n = 1, \dots, 5$ ). The 26 data maps contain a total of 8804 potential data. Uncorrelated Gaussian noise having standard deviation 5% of the total potential is added to each datum.

Both AIM-MS and AIM-DS inversions of this data set are given by *Li and Oldenburg [1994]*. The AIM-MS results are reproduced here. The same finite difference code used in the CG example was used for forward modeling. The mesh contained 17,496 cells ( $27 \times 27 \times 24$ ). The convergence curves for the inversion are shown in Figure 6. A steady reduction of the misfit is observed in Figure 6a, and the expected misfit of 8804 is achieved after four iterations. Figures 6b and 6c show the norm of the model and the model perturbation for successive iterations. The model recovered at the fourth iteration is shown in Plate 3. Comparison of the inverted results with the true cross sections in Plate 2 shows that all conductivity anomalies have been recovered and the dynamic range is comparable with that in the true model. There is good correspondence between the results from the CG inversion in Plate 2

and the AIM results in Plate 3. Differences are expected, however; the AIM-MS inversion does not minimize a specific model objective function, and smoothness is incorporated into the inversion by limiting the wavenumbers at which the one-dimensional inversions are carried out. Also, the data used in the AIM inversion have 5 times the error as those in the CG inversion. We emphasize that the inversion result in Plate 3 was produced with only five forward modelings.

## 7. Summary

The purpose of this paper is to outline various strategies for coping with large-scale EM inverse problems. If computing power were not an issue, then a traditional Gauss-Newton approach would be the method of choice. This requires computation of the sensitivity matrix, solving a large system of equations, and carrying out a line search using forward modeling. The subspace method reduces the computations by projecting the large system of equations onto a much smaller subspace and then inverting only a small matrix. Selection of basis vectors for the subspace method is crucial, but the strategy of using steepest descent vectors associated with partitioned model and data misfit objective functions has worked well for us. Our experience with subspace and Gauss-Newton approaches is that approximate sensitivities will often suffice; this has the potential for further computational reduction in the subspace approach.

In the conjugate gradient approach one does not need to compute and store the full sensitivity matrix. Only the gradient of the objective function, which requires forward modeling, need be calculated. There is no matrix to invert, but a line search, involving forward modeling, is needed to compute the scaling factor for the perturbation. Because only a single vector is used in the perturbation, it is important that the gradient vector is computed accurately. Also, with the conjugate gradient method the value of the Lagrange multiplier must be supplied explicitly. This can be accomplished by monitoring the convergence process and adjusting the Lagrange multiplier when plateauing occurs.

The AIM procedure involves the least computation, requiring no computation of sensitivities or solution of a matrix system. It produces an updated model by performing only one forward modeling per iteration. The trade-off for this computational

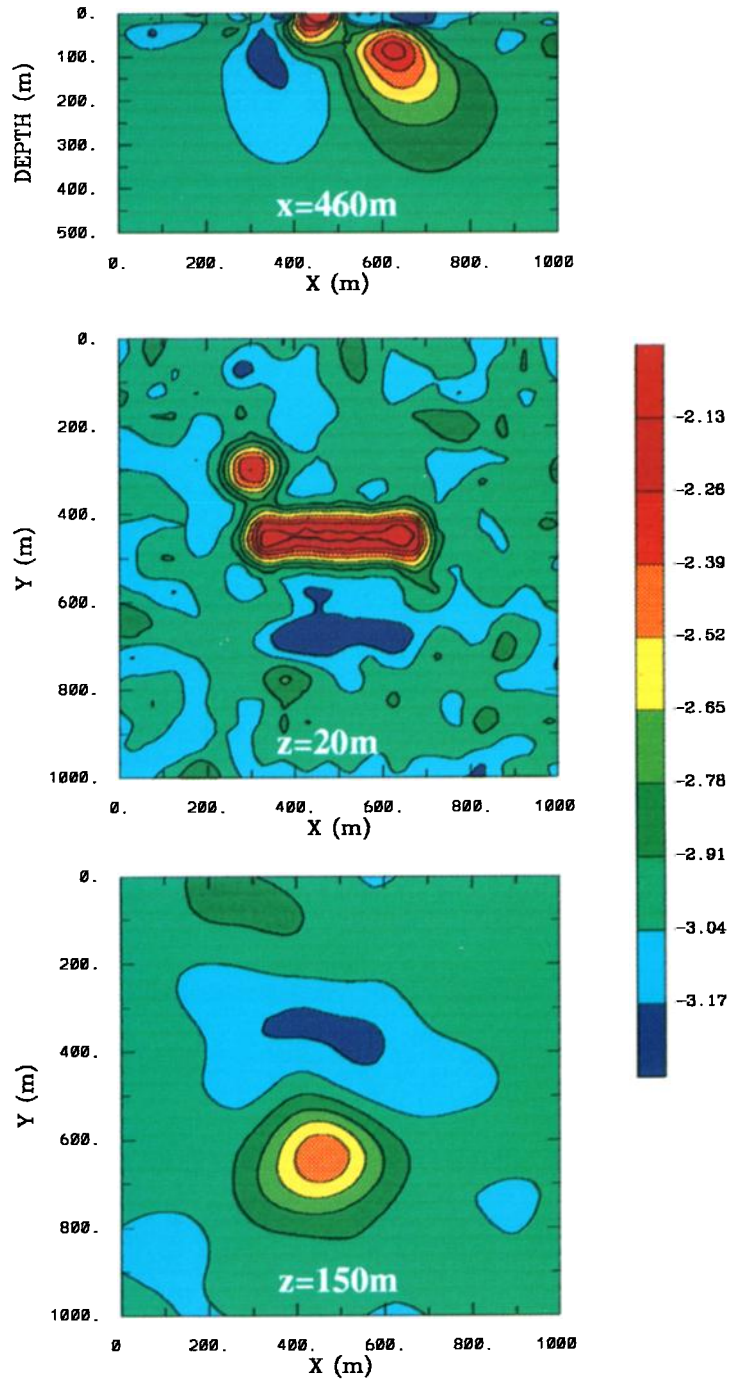


**Plate 3.** The conductivity model recovered from the fourth iteration of an AIM-MS inversion of data from the five-prism model. (top) Vertical section through the model at  $x = 460$  m. (middle) Horizontal section at  $z = 20$  m. (bottom) Horizontal section at  $z = 150$  m. The color bar shows  $\log_{10} \sigma$  and applies to all panels. This is considered to be the final model since the expected  $\chi^2$  misfit is achieved. The model sections can be compared with the true sections in Plate 2.

efficiency is a potential loss of robustness and possible lack of control upon the final model. The characteristics of the recovered model are intimately associated with the details of the approximate inverse mapping operator. Our experience with the AIM-MS and AIM-DS procedures outlined here is that a few applications generally produce substantial reduction in data misfit and, depending upon the details of the inverse mapping, produce a model with desirably smooth features. With successive iterations the algorithm may diverge, but the minimum misfit model, or one of the models achieved as the inversion has proceeded, may be interpretable in itself or used as a starting model in a more sophisticated inversion.

Each attempt to reduce the number of computations in the inversion has the potential for producing an algorithm which has its own difficulties with respect to getting trapped in a local minimum, requiring additional iterations for convergence, losing ability to directly control the characteristics of the inverted model, or having decreased robustness. Nevertheless, the task of the inverter is to process his/her data so that some inferences about model structure can be made. The work presented here outlines some strategies such that a user, when confronted with inverting EM data, can choose an attack which produces optimum results given the limitations of computing power and storage.

**Acknowledgments.** The author is grateful to Rob Ellis, Yaoguo Li, and Peter McGillivray for their contributions to the conjugate gradient, approximate inverse mapping, and subspace techniques that have been presented in this paper. Funding for this research has been provided by an NSERC grant 5-84270, and also through an NSERC-Industry Consortium, "Joint/Cooperative Inversion of Geophysical and Geological Data" with industrial partners: Placer Dome, Cominco Exploration, Noranda Exploration, BHP Minerals, HBE&D, INCO Exploration and Technical Services, Falconbridge (Limited) Exploration, Newmont Gold Company, Kennecott Exploration, WMC, and CRA Exploration.

## References

- deGroot-Hedlin, C., and S. Constable, Occam's inversion to generate smooth, two-dimensional models from magnetotelluric data, *Geophysics*, 52, 289–300, 1990.
- Dey, A., and H. F. Morrison, Resistivity modelling for arbitrary shaped two-dimensional structures, *Geophys. Prospect*, 27, 106–136, 1979a.
- Dey, A., and H. F. Morrison, Resistivity modelling for arbitrary shaped three-dimensional structures, *Geophysics*, 44, 753–780, 1979b.
- Ellis, R. G., and D. W. Oldenburg, Magnetotelluric inversion using Green's functions and conjugate gradients, *Geophys. J. Int.*, in press, 1994a.
- Ellis, R. G., and D. W. Oldenburg, The pole-pole 3d dc resistivity inverse problem: A conjugate gradient approach, *Geophys. J. Int.*, in press, 1994b.
- Gill, P. E., W. Murray, and M. H. Wright, *Practical Optimization*, 401 pp., Academic, San Diego, Calif., 1981.
- Habashy, T. M., R. W. Groom, and B. R. Spies, Beyond the Born and Rytov approximations: A nonlinear approach to electromagnetic scattering, *J. Geophys. Res.*, 98, 1759–1775, 1993.
- Hestenes, M. R., *Conjugate Directions Methods in Optimization*, 324 pp., Springer-Verlag, New York, 1980.
- Hohmann, G. W., Three-dimensional induced polarization and electromagnetic modeling, *Geophysics*, 40, 309–324, 1975.
- Lanczos, C., *Linear Differential Operators*, Van Nostrand Reinhold, New York, 1961.
- Lee, T., An integral equation and its solution for some two- and three-dimensional problems in resistivity and induced polarization, *Geophys. J. R. Astron. Soc.*, 42, 81–95, 1975.
- Li, Y., and D. W. Oldenburg, Approximate inverse mappings in dc resistivity problems, *Geophys. J. Int.*, 109, 343–362, 1992.
- Li, Y., and D. W. Oldenburg, Inversion of 3D dc resistivity data using an approximate inverse mapping, *Geophys. J. Int.*, in press, 1994.
- Madden, T. R., Inversion of low frequency electromagnetic data, in *Oceanographic and Geophysical Tomography*, edited by Y. Desaubies, A. Tarantola, and J. Vinn-Justin, pp. 379–408, North-Holland, New York, 1990.
- Madden, T. R., and R. L. Mackie, Three-dimensional magnetotelluric modeling and inversion, *IEE Proc. Part H: Microwaves Opt. Antennas*, 77, 318–333, 1989.
- McGillivray, P. R., Forward modeling and inversion of dc resistivity and MMR data, Ph.D. thesis, Dep. of Geophys. and Astron., Univ. of British Columbia, Vancouver, Can., 1992.
- McGillivray, P. R., and D. W. Oldenburg, Methods for calculating Fréchet derivatives and sensitivities for the nonlinear inverse problem: A comparative study, *Geophys. Prospect.*, 38, 499–524, 1990.
- McGillivray, P. R., D. W. Oldenburg, R. G. Ellis, and T. M. Habashy, Calculation of sensitivities for the frequency domain electromagnetic problem, *Geophys. J. Int.*, 116, 1–4, 1994.
- Morse, P. W., and H. Feshbach, *Methods of Theoretical Physics*, McGraw-Hill, New York, 1953.

- Oldenburg, D. W., Inversion of electromagnetic data: An overview of new techniques, *Surv. Geophys.*, *11*, 231–270, 1990.
- Oldenburg, D. W., and R. G. Ellis, Inversion of geophysical data using an approximate inverse mapping, *Geophys. J. Int.*, *105*, 325–353, 1991.
- Oldenburg, D. W., and R. G. Ellis, Efficient inversion of magnetotelluric data in two dimensions, *Phys. Earth Planet. Inter.*, *81*, 177–200, 1993.
- Oldenburg, D. W., and Y. Li, Subspace linear inverse methods, *Inverse Probl.*, in press, 1994.
- Oldenburg, D. W., P. R. McGillivray, and R. G. Ellis, Generalized subspace methods for large scale inverse problems, *Geophys. J. Int.*, *114*, 12–20, 1993.
- Paige, C. C., and M. A. Saunders, LSQR: An algorithm for sparse linear equations and sparse least squares, *ACM Trans. Math. Software*, *8*, 43–71, 1982.
- Park, S. K., Inversion of magnetotelluric data for multi-dimensional structure, *Rep. 87/b*, Inst. of Geophys. and Planet. Phys., Los Angeles, Calif., 1987.
- Park, S. K., and G. P. Van, Inversion of pole-pole data for 3-D resistivity structure beneath arrays of electrodes, *Geophysics*, *56*, 951–960, 1991.
- Pelton, W. H., L. Rijo, and C. M. Swift, Jr., Inversion of two-dimensional resistivity and induced polarization data, *Geophysics*, *43*, 788–803, 1978.
- Polyak, E., and G. Ribiere, Note sur la convergence des méthodes conjuguées, *Rev. Fr. Inr. Rech. Oper.*, *16*, 35–43, 1969.
- Press, W. H., S. A. Teukolsky, W. T. Vetterling, and B. P. Flannery, *Numerical Recipes in Fortran*, 2nd ed., Cambridge University Press, New York, 1992.
- Ramirez, A., W. Daily, D. LaBrecque, E. Owen, and D. Chesnut, Monitoring an underground steam injection process using electrical resistance tomography, *Water Resour. Res.*, *29*, 73–87, 1993.
- Roach, G. F., *Green's Functions*, 325 pp., Cambridge University Press, New York, 1982.
- Sasaki, Y., Two-dimensional joint inversion of magnetotelluric and dipole-dipole resistivity data, *Geophysics*, *54*, 254–262, 1989.
- Smith, N. C., and K. Vozoff, Two-dimensional dc resistivity inversion of dipole-dipole data, *IEEE Trans. Geosci. Remote Sens.*, *22*, 21–28; 1984.
- Tripp, A. C., G. W. Hohmann, and C. M. Swift, Jr., Two-dimensional resistivity inversion, *Geophysics*, *49*, 1708–1717, 1984.
- Weidelt, P., Inversion of two-dimensional conductivity structures, *Phys. Earth Planet Inter.*, *10*, 282–291, 1975.
- Whittall, K. P., and D. W. Oldenburg, *Inversion of Magnetotelluric Data Over a One-Dimensional Conductivity*, Geophys. Monogr. Ser., vol. 5, edited by David V. Fitterman, Soc. of Explor. Geophys., Tulsa, Okla., 1992.

---

D. W. Oldenburg, UBC–Geophysical Inversion Facility, Department of Geophysics and Astronomy, University of British Columbia, Vancouver, British Columbia, Canada V6T 1Z4.

(Received July 29, 1993; revised March 2, 1994; accepted March 2, 1994.)